



Title	The Applications of Acoustic Emission Methods to Forecasting of the Rock and Gas Outburst in Coal Mine
Author(s)	Watanabe, Yoshiteru; Nakajima, Iwao; Takeuchi, Masayuki; Maebara, Tatsuya
Citation	Memoirs of the Faculty of Engineering, Hokkaido University, 15(2), 187-198
Issue Date	1979-12
Doc URL	http://hdl.handle.net/2115/37982
Type	bulletin (article)
File Information	15(2)_187-198.pdf



[Instructions for use](#)

The Applications of Acoustic Emission Methods to Forecasting of the Rock and Gas Outburst in Coal Mine

**Yoshiteru WATANABE* Iwao NAKAJIMA*
Masayuki TAKEUCHI* Tatsuya MAEBARA***

(Received June 30, 1979)

Abstract

The acoustic emission activities accompanying the rock and gas outbursts were observed during a cross-measure drivage at Horonai Coal Mine. In practice, two outbursts which occurred after blasting were monitored successfully. The mechanism of the outburst occurrence was considered and the possibility of forecasting them was discussed on the basis of the observational results.

Actually, the acoustic emission activity after blasting became remarkably at a high degree prior to outburst when the outburstprone seam was exposed by a working face. Consequently, it was confirmed that the impending outburst could be forecasted with a high probability by monitoring the degree of an increase in acoustic emission activity after blasting. Furthermore, these observational results provided a new interpretation for the process of the outburst occurrence.

1. Introduction

Since the incident of a gas explosion due to the rock and gas outburst at Horonai Coal Mine in 1975, outbursts have been becoming a serious problem on account of a high degree of hazard at some coal mines in Hokkaido. Generally, this type of rock and gas outburst occurs immediately after blasting in driving of a certain seam which consists of relatively porous sandstones. In the occurrence of this outburst, the sandstones scaled off are rapidly ejected from the solid with a large volume of firedamp smacking of petroleum. The hazardous zones of the outburst can be identified by considering geologically the outburst-prone seam of the sandstone in which the outbursts occurred in past. But the methods for forecasting exactly an impending outburst are not found at the present stage.

Recently, the acoustic emission technique has attracted special interest as a method for actually monitoring the process of a rock failure in the field of mining engineering. The primary objective of this research is to clarify whether the acoustic emission technique is useful as a method for forecasting the occurrence of this type of rock and gas outburst. In order to carry out this objective the acoustic emission activity of rock during the drivage of a roadway at intersections with the

*) Department of Resources Development Engineering, Faculty of Engineering, Hokkaido University, Sapporo, 060, Japan.

outburstprone seam was observed with sufficient sensitivity for practical use at Horonai Coal Mine in 1978.

During the observations, the incident of the rock and gas outbursts occurred two times and the acoustic emission activities accompanied by them were recorded successfully. Consequently, it was recognized that the fracturing activity in the outburst-prone sandstone increased markedly prior to the outburst, and that the acoustic emission method allowed for an early detection of the state of the rock and gas outburst hazard.

2. Description of outburst and working in drivage

The acoustic emission activity of rock ahead of working faces was observed during the cross-measure drivage of No. 2 roadway at the intersection with the outburst-prone seam of the sandstone. This roadway is at the seventh level of which the depth reached about 1055 m.

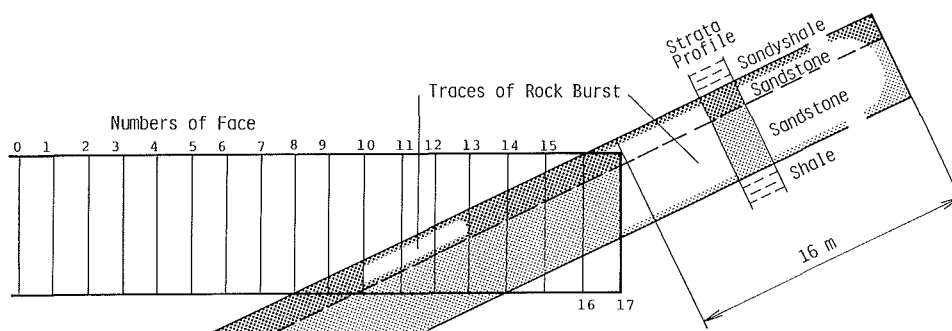


Fig. 1. Numbers of face advanced and strata profile.

Fig. 1 shows the longitudinal section of No. 2 roadway and the traces of the outburst in the cross-measure drivage. In addition, Fig. 1 presents the strata profile of the outburst-prone seam having an inclination of 25 degrees. The outburst-prone seam consists of such rocks as sandys shale, coarse-grained sandstone and medium-grained sandstone and shale in the order of the upper seam to the lower. The seams of the coarse-grained sandstone and the medium-grained sandstone are 0.8 and 2.0 m in thickness respectively. The uniaxial compressive strength and the porosity of the coarse-grained sandstone are 785 kg/cm² and 5%, and those of the medium-grained sandstone are 1100 kg/cm² and 2% respectively.

During the observations, two rock and gas outbursts occurred in this outburst-prone seam. The first outburst occurred only in the seam of the coarse-grained sandstone when it was exposed in the floor of working face. The second outburst occurred in both sandstone seams when they appeared in the roof of face. Fig. 2 is the ground plane of the traces of the outbursts occurred in the drivage of No. 1 and No. 2 roadway. In Fig. 2, A and B are the traces of the first outburst and the second occurred during the drivage of No. 2 roadway, while C and

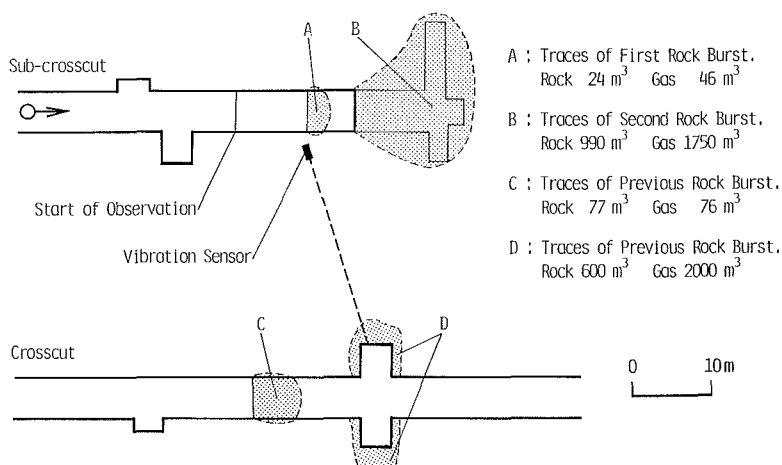


Fig. 2. Arrangement of vibration sensor for detection of acoustic emission during driving in HORONAI Coal Mine.

D are those of the outbursts occurred during the drivage of No. 1 roadway previously. Among these traces, D is the outburst which induced the incident of a gas explosion mentioned at the beginning. The outburst of A was small in scale, and discharged 4 m³ of rock and 46 m³ of gas over a short time. The outburst of B was large in scale, and discharged 400 m³ of rock and 1750 m³ of gas. The volume of the crushed zone was 24 m³ in the case of A and 990 m³ in the case of B.

Before the drivage of No. 2 roadway, 10 relief boreholes of 90 mm in diameter and 70 m in depth were drilled in the direction of the advance as a preventive measure for the outburst. These boreholes were arranged in such a way as to have the roadway surrounded with them at the section ahead of 70 m from a face. After boring the gas pressure in each boreholes was kept as high as atmospheric pressure. So by a vacuum pump, gas amounting to 3000 m³ was drawn out from these boreholes. In the drivage, 87 shotholes were arranged for a face of 18.5 m², and were charged with 25 kg of permissible explosive. In practice, MS-delay blasting of 8-row rounds was carried out with pyramid cut. The advance of the face per shift is 0.7 m.

3. Methods of observation of acoustic emission activity

Fig. 3 presents a block diagram of the acoustic emission monitoring system used in the observation at this time. This original system consists of a basic two-channel system, and includes two vibration sensors, two preamplifiers, an acoustic emission instrumentation which accept two-input and a real-time spectrum analyzer. Additionally, this monitoring system is similar to that used at Sunagawa Coal Mine, so the reader may refer to the previous report¹⁾ for details.

The vibration sensor has a high sensitivity of 250 mV/g and a flat frequency

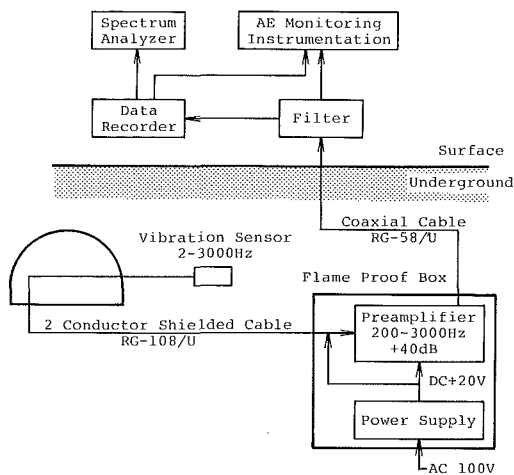


Fig. 3. Overall acoustic emission monitoring system.

response from 2 to 3000 Hz. It was cemented into the bottom of a borehole prepared in the solid rock near No. 2 roadway before driving as shown in Fig. 2. In this case, a borehole of 90 mm in diameter and 28 m in depth was drilled from No. 1 roadway in the direction of the intersection of the outburst-prone seam and the extension of No. 2 roadway. In Fig. 2, the sensor was connected to the preamplifier, which was placed within a flame-proof box, with two-conductor shielded cable of about 250 m in length. The circuit between the sensor and the preamplifier, which were powered by the source of DC 18 V, was intrinsically safe. Between the flame-proof box underground and the acoustic emission instrumentation on the surface, a coaxial cable of about 2500 m in length was installed through roadways, an inclined shaft and a vertical shaft. Acoustic emission signals detected by the sensor were amplified by the preamplifier which has a fixed gain of 40 dB, and were transmitted as the input-signals of acoustic emission instrumentation. Besides, the output impedance of $50\ \Omega$ was provided with the amplifier to prevent electrical interference in the transmission over a long distance.

The acoustic emission instrumentation which was made by Dunegan/Endevco, allowed for a satisfactory analyzation of the parameters associated with acoustic emission activity such as count rate, accumulated events and accumulated relative energies with real time. Here, the count rate is the number of acoustic emission pulses exceeded a threshold level per unit time. Accumulated events are the total number of the train of the pulses, and accumulated relative energies are the sum of the mean square of the pulses²⁾. These parameters are dependent on the sensitivity and the signal to noise ratio of the monitoring system but also are dependent on the frequency response of the overall. For this reason, acoustic emission signals were recorded on a magnetic tape if necessary, and their wave forms and frequency spectra were analyzed by the spectrum analyzer made by Nicolet. Practically, these analytical results gave the optimum conditions such as frequency band, a gain of amplification and a threshold level in analyzing the parameters associated

with the acoustic emission activity.

Recently, K. Mogi³⁾ indicated that the amplitude-frequency distribution of acoustic emissions depended both on the structural states of rock mass and the stress state in medium. On the basis of his standpoints, the analyses of the amplitude-frequency distribution of acoustic emissions recorded were tried by the distribution analyzer set in the instrumentation.

4. Interpretation of records of acoustic emission signals

Fig. 4 presents two typical acoustic emission signals, which were recorded through the band-pass filter of 300~3000 Hz, and their frequency spectra. For this reason both the signals are primarily composed of a frequency content in the range of 300~3000 Hz. The dominant frequency is 1012 Hz in the signal of *L* and 2500 Hz in the signal of *H*. The signals with approximately 2500 Hz of dominant frequency were more in number among the acoustic emission signals recorded. In Fig. 4 the level of background noises is negligibly low in comparison with that of the signals. Such analytical results gave the optimum conditions for processing acoustic emission signals recieved.

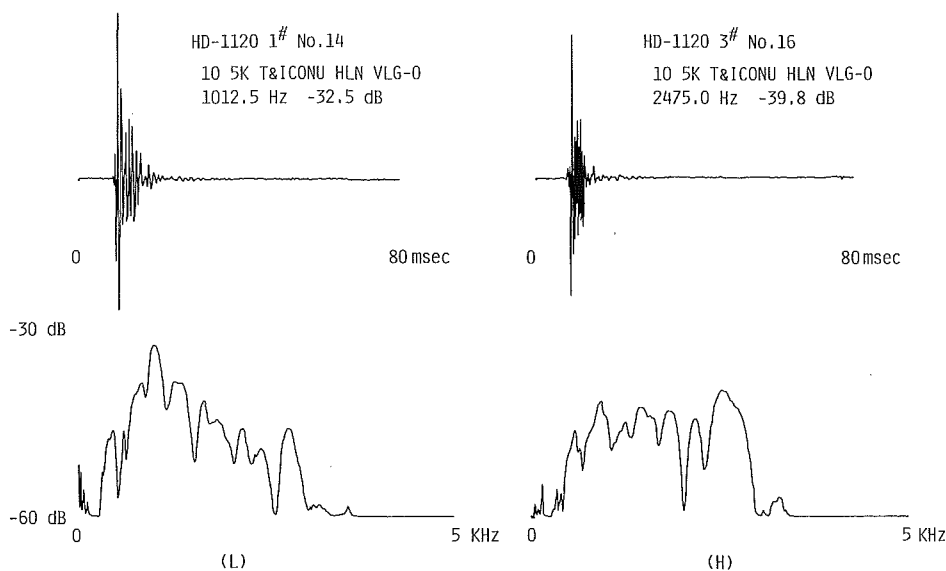


Fig. 4. Typical acoustic emission signals and their frequency spectra.

Fig. 5 shows the blasting signals and the acoustic emission signals occurred immediately after blasting. The numbers marked in Fig. 5 correspond to those in Fig. 1 which indicate the position of the working faces in the cross-measure drive of No. 2 roadway. At the face of No. 1 no acoustic emissions are found within 500 milli-seconds after blasting except blasting signals. At the blastings of the sandyshale between No. 0 and No. 8 their signals showed a similar form to No. 1. At the face of No. 9, where the coarse-grained sandstone in the outburst-

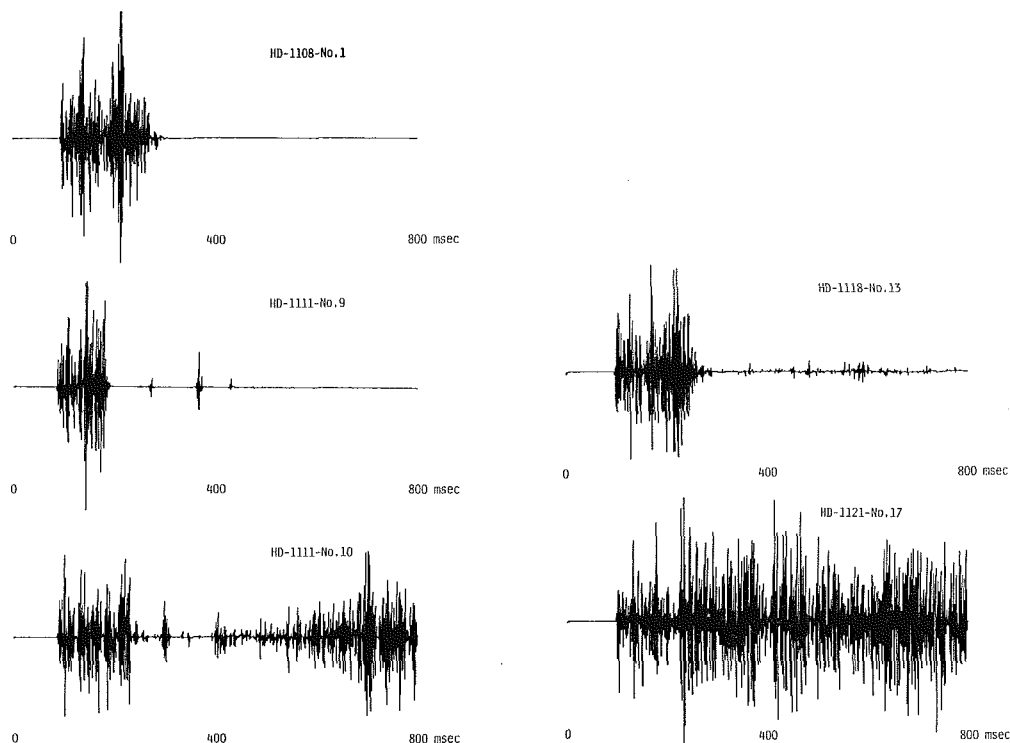


Fig. 5. Signals of blasting and acoustic emission.

prone seam were exposed in the floor, a few acoustic emissions are found immediately after blasting. The first rock and gas outburst occurred at the blasting of No. 10. In this case the onset of the outburst occurs after about 150 milliseconds from the blasting, and becomes active with the lapse of time. Successive acoustic emissions of low level were noted at the blasting of No. 13. The second outburst occurred at the blasting of No. 17, where the coarse-grained sandstone appeared in the roof. In this case the outburst triggers violent action simultaneously with the last round of the blasting. Such an outburst is highly hazardous for gas explosion, if the explosives of the last rounds are fired imperfectly in a firedamp-air mixture.

5. Acoustic emission activity in the process of the outburst occurrence

In the cross-measure drivage of No. 2 roadway acoustic emission activity at each working face was monitored for about 30 minutes after blasting. Fig. 6 presents the charts of count rate and accumulated events recorded with real time.

In the blasting of only the sandyshale at No. 7 and No. 8 both the values of count rate and the number of events are small. The curve of accumulated events becomes flatter within a few minutes. But at the face of No. 9, where

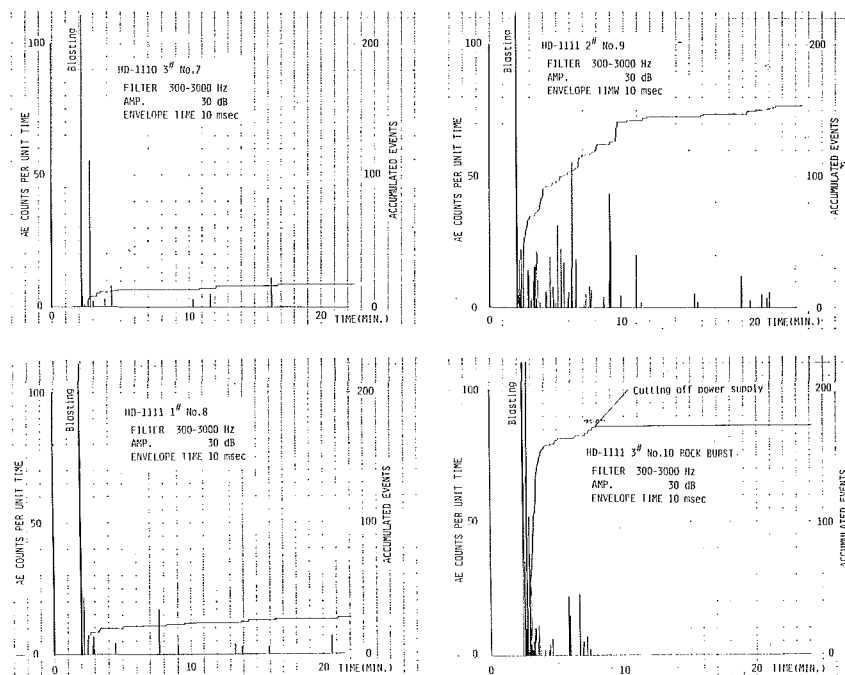


Fig. 6. Acoustic emission activity after blasting in driveage.

the coarse-grained sandstone was exposed on the floor, the acoustic emission activity is remarkably at a high degree in comparison with that at No. 7 and No. 8. In this chart a high count rate is recorded successively for about 10 minutes after blasting. The curve of accumulated events steepens rapidly immediately after blasting, and becomes flatter with the lapse of time. At the blasting of No. 10 the acoustic emission activity increases abnormally immediately after blasting corresponding to the occurrence of the first outburst. In this case the monitoring of acoustic emission was interrupted after 6 minutes from blasting because the underground power supply was cut off by an interlocker connected with a detector of methane.

Fig. 7 and Fig. 8 show the accumulated values of acoustic emission counts, events and relative energies per 30 minutes and 5 minutes respectively after blasting at each face of the cross-measure driveage.

The numbers marked in these figures correspond to those of the faces in Fig. 1. In each figure the acoustic emission activity was at a low degree at the faces limited to sandy shale between No. 0 and No. 8. When the coarse-grained sandstone seam was exposed on the floor of No. 9, the values of each parameter increased extraordinarily, and at the next blasting the first outburst occurred in that seam as shown in Fig. 1. After that the activity was at a considerably high degree in the face of No. 12 in spite of the surviving of the crushed zone due to the first outburst. With the advance of the face from No. 13 into the undisturbed region the activity increased again and reached a peak at the face of No. 15. The state

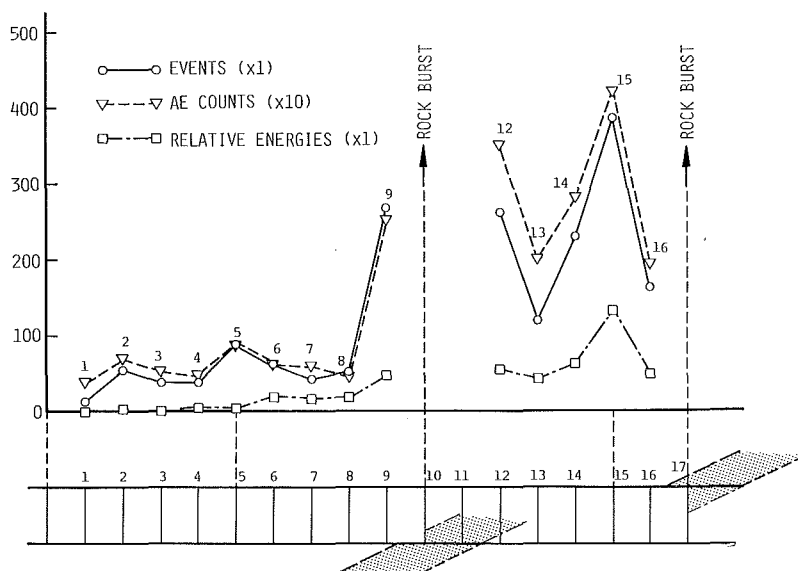


Fig. 7. Variation of AE activity per 30 minutes with advance of working face in drivage.

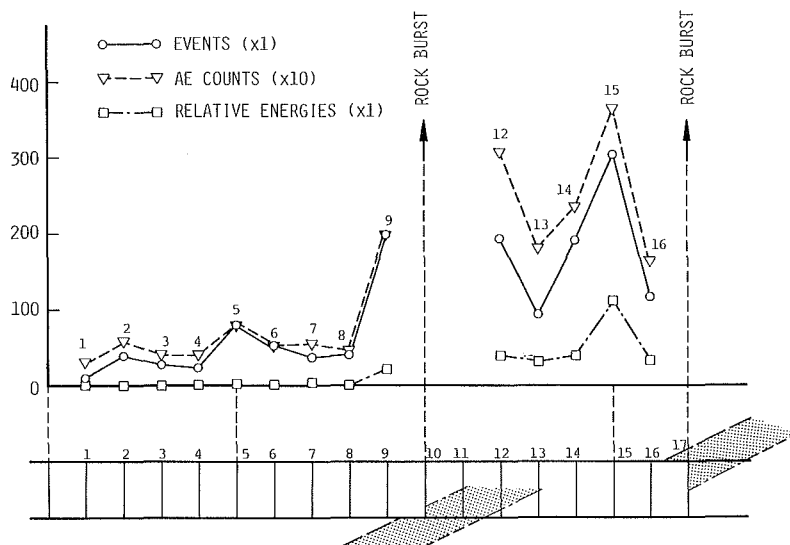


Fig. 8. Variation of AE activity per 5 minutes with advance of working face in drivage.

of the activity at that time is illustrated in Fig. 9 with the curves of acoustic emission counts, events and relative energies accumulated with the lapse of time after blasting. Each curves steepen extremely immediately after blasting and after about 3 minutes. Such a violent activity appears to indicate that the outburst was impending at that time. At the next blasting the activity decreased once, and the

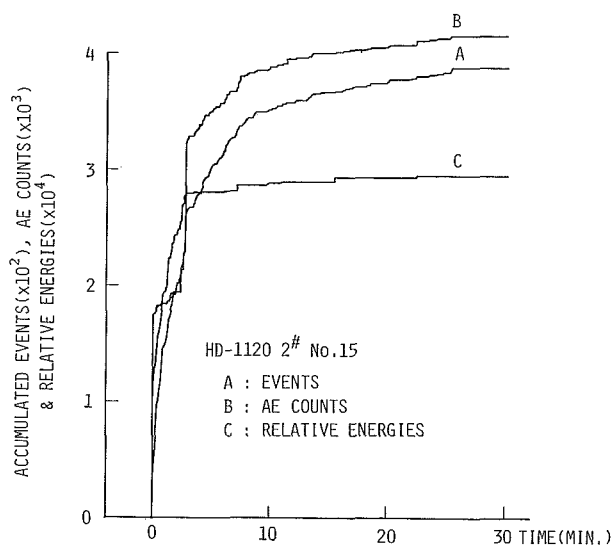


Fig. 9. Acoustic emission activity after blasting.

second outburst occurred simultaneously with the blasting of No. 17 where the outburst-prone seam appeared at the roof. As above mentioned, there is little difference between the observational results of the acoustic emission activities for 30 and 5 minutes after blasting. Consequently, the degree of the activities can be sufficiently estimated by the observation for only 5 minutes after blasting.

From the observational results above mentioned, it is suggested that there are two types in the phase of acoustic emission activity occurring prior to the outburst. Namely, one is the type of the first outburst which succeeded the increase in the activity, extraordinarily exceeding the average level for that observed previously. The other is the type of the second outburst which occurred after a decrease in the activity maintained at a high degree previously.

According to the observational results¹⁾ obtained in deeplevel mining at other coal mines to date, the charts of acoustic emission activity after blasting showed such a pattern as seen at No. 7 and No. 8 in Fig. 6 in the drivage of solid rock, while such a pattern as No. 9 in Fig. 6 and No. 15 in Fig. 9 was seen in the case of rock including a geologically weak band. This indicates that in solid rock a few fractures originate at the stress level induced in the process of stress redistribution after blasting, and that in weak rock many fractures originate at that stress level. Besides, the higher the fracturing activity, the longer the time required for the rock surrounding and adjacent to faces to attain equilibrium again. On the basis of this standpoint, the seams of the coarse-grained sandstone and the medium-grained sandstone are considered to be a geologically friable band beyond one's expectation.

The friability of the outburst-prone seam seems to be due to the stress concentration at the structural heterogeneities in rock. The reasonableness of this remark are also suggested by the analytical results of the amplitude-frequency dis-

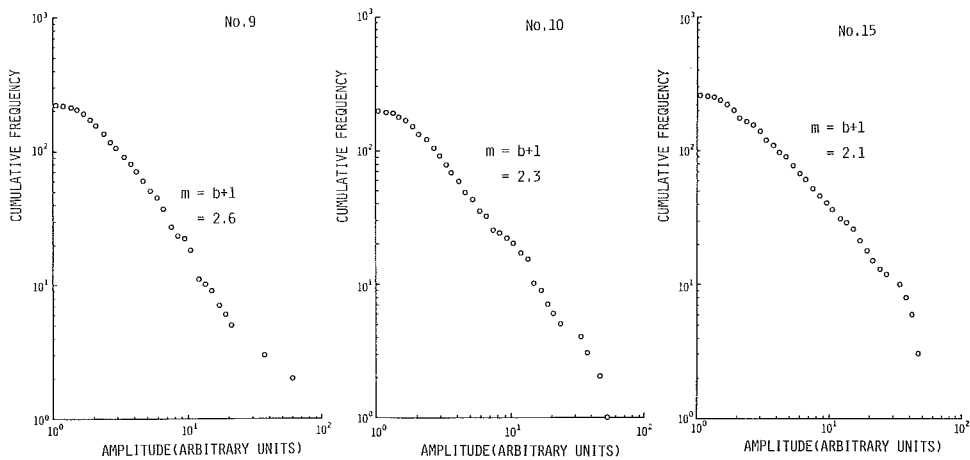


Fig. 10. Amplitude-frequency distribution of acoustic emission.

tribution of acoustic emissions as shown in Fig. 10. Fig. 10 presents those of acoustic emission occurring for 30 minutes after blasting in the face of No. 9, No. 10 and No. 15. These distributions could be expressed by the following equation, which is referred to the Ishimoto-Lida distribution in seismology.

$$n(a) da = ka^{-m} da$$

where a is the maximum trace amplitude of acoustic emissions, $n(a)da$ is the number of events within the interval from a to $a+da$, and k and m are both constants. In each distribution, it is found that the exponent m is very large in the range between 2.1 and 2.6. According to K. Mogi, the exponent m increases with the degree of the stress concentration at the structural heterogeneities in the medium. On the basis of his concluding remarks, the medium in the outburst-prone seam may be under the spatial variation in the stress distribution. It appears to be for this reason that the frequency of the occurrence of small fracture in scale is high in each case of Fig. 10.

6. Possibility of forecasting of an impending outburst

Regarding the consideration of the acoustic emission activities in the process of occurrence of this type of rock and gas outburst, its mechanism generally is as follows; in the rock ahead of the face of drivage the change in stresses induced after blasting should become large in proportion to rock pressure. The degree of fracturing activities occurring prior to the outbursts depends on this change in stresses and the strength of the rock. Actually, the high fracturing activities as shown at No. 9 in Fig. 6 or at No. 15 in Fig. 9 are considered to occur densely in outburst-prone seam exposed by the working face, especially in the crushed zone which is formed in the outburst-prone seam. Consequently, a number of cracks are accumulated in that zone prior to the outburst. On account of the change in the sorption and filtration properties of the rock for gas with the cumulation of

cracks, the crushed zone is saturated with free gas under high pressure. At this stage the blasting triggers the outburst.

To date this type of rock and gas outburst has been considered to occur instantaneously after blasting without any warning signs. But, according to the observational results obtained in this study, the acoustic emission activity accompanying the outburst triggers the action by the previous blast. As a results of the considerations on the mechanism of the outburst occurrence, the forecasting appears to be possible if the degree of the cumulation of cracks in the rock ahead of face is estimated by monitoring acoustic emission activity. Especially, sufficient information to forecast the impending outburst could be obtained from the observational results only 5 minutes after blasting because the high acoustic emission activity occurs in the process of the stress redistribution.

7. Concluding remarks

As mentioned above, the acoustic emissions which occurred in the rock ahead of the face during a cross-measure drivage were observed with real time at Horonai Coal Mine. During the observations, the acoustic emission activities accompanying the rock and gas outbursts were monitored two times successfully. The mechanism of the outburst occurrence was considered on the basis of these observational results. Consequently, the following conclusions can be drawn;

(1) When a certain sandstone seam is exposed by the working face, the acoustic emission activity after blasting becomes remarkably intense. On the basis of this result, the sandstone seam can be identified as the outburst-prone seam.

(2) The outburst occurrence can be forecasted with a high probability by monitoring the degree of an increase in acoustic emission activity after blasting.

(3) There are two types in acoustic emission activity prior to the outburst. One is the type in which the outburst succeeds to increase in the acoustic emission activity, and the other is the type in which it occurs after a decrease in the acoustic emission activity which was maintained at a high degree previously.

(4) The analytical results of the amplitude-drequencey distribution of acoustic emission seem to indicate that the medium in the outburst-prone seam is conspicuously under spatial variation in the stress distribution.

(5) Each outburst occurred when the outburst-prone seam was exposed by the corners of the cross-measure drivage. One of these outbursts occurred at the floor of face after about 150 milliseconds and another at the roof simultaneously with the last round of the blasting.

Acknowledgement

The authors wish to thank Mr. Tetsu Fukai for valuable suggestions and Mr. Kenichi Itakura for assistance in the work. This work was supported in part by a research grant of THE COAL MINING RESEARCH CENTRE, JAPAN.

References

- 1) Watanabe, Y. and I. Nakajima: Acoustic Emission Activity in Bed Rock Surrounding Underground Working Faces in Deeplevel Coal Seams, *Memories of Engineering, Hokkaido Univ.*, XV (1978), 1 (66), p. 1-18.
- 2) Hardy, H. R. Jr: Application of Acoustic Emission Techniques to Rock Mechanics Research, American Society for Testing and Materials, (1972).
- 3) Mogi, K., Magnitude-Frequency Relation for Elastic Shocks Accompanying Fractures of Various Materials and Some Related Problems in Earthquakes (2nd Paper), *Bull. Earthq. Res. Inst.*, 40 (1962), p. 831-853.